Bioelectrochemistry 82 (2011) 29–37

Contents lists available at ScienceDirect

Bioelectrochemistry

journal homepage: www.elsevier.com/locate/bioelechem

Assessing multidrug resistance protein 1-mediated function in cancer cell multidrug resistance by scanning electrochemical microscopy and flow cytometry

Sabine Kuss [a,b], Renaud Cornut [a], Isabelle Beaulieu [a], Mohamed A. Mezour [a], Borhane Annabi [b], Janine Mauzeroll [a,*]

[a] Laboratory for Electrochemical Reactive Imaging and Detection for Biological Systems, Department of Chemistry, Université du Québec à Montréal, C.P. 8888, Succ. Centre-ville, Montréal, QC, Canada H3C 3P8

[b] Molecular Oncology Laboratory, Department of Chemistry, BioMED Research Centre, Université du Québec à Montréal, C.P. 8888, Succ. Centre-ville, Montréal, QC, Canada H3C 3P8

ARTICLE INFO

Article history:
Received 16 September 2010
Received in revised form 28 March 2011
Accepted 21 April 2011
Available online 5 May 2011

Keywords:
Multidrug resistance
Scanning electrochemical microscopy
Glutathione
Flow cytometry

ABSTRACT

Cancer cell multidrug resistance is a molecular signature that highly influences the outcome of chemotherapy treatment and for which there is currently no robust method to monitor *in vitro* its activity. Herein, we demonstrate that ferrocenemethanol ($FcCH_2OH$) and its oxidized form ($[FcCH_2OH]^+$) affect the redox state of cancer cells. Specifically, the interaction of $FcCH_2OH$ with the glutathione couple (GSH/GSSG) is shown in human adenocarcinoma cervical cancer cells HeLa and a multidrug resistant variant overexpressing the multidrug resistant associated protein 1 (MRP1) using bioanalytical techniques, such as flow cytometry and fluorescence microscopy. It is further demonstrated that the differential response to $FcCH_2OH$ in multidrug-resistant cells is in part due to MRP1's unspecific efflux. Scanning electrochemical microscopy confirmed the interaction between $FcCH_2OH$ and the cells, and the differential response was observed to depend on MRP1 expression. This newly established relation between $FcCH_2OH/[FcCH_2OH]^+$, GSH/GSSG and multidrug resistance in human cancer cells enables than the acquisition of scanning electrochemical microscopy images.

1. Introduction

Cancer cells actively defend themselves through multidrug resistance. Such cellular and molecular signature in many different cancer types, including acute leukemia, colon, kidney, pancreas, and carcinoid cancers, seriously undermines the success of chemotherapeutical treatments [1]. For example, it is estimated that out of 7000 new ovarian cancer patients annually in Canada and the US, 70% of them will exhibit resistance to treatment such as their survival rates decline to 10–30% [2].

The decrease in sensitivity against chemotherapeutic agents in resistant tumor cells is closely related to the action of non-selective transmembrane proteins that actively remove the agents from inside the cells [3]. In the present study, the contribution of the multidrug resistance protein 1 (MRP1) is specifically evaluated through the action of two human cervical adenocarcinoma cancer cell lines: a HeLa cell line (HeLa) and a multidrug-resistant variant, overexpressing MRP1 (HeLa-R). MRP1 is known to transport, among others, glutathione (GSH) and drugs conjugated to GSH out of the cell [4]. Alterations in the GSH levels, in GSH s-transferase (GST) levels and its activity, have been reported to affect cellular resistance to chemotherapeutic agents such as anthracyclines and cisplatin [5]. More recently, there has been a growing interest in the search for new antitumor compounds that do not interact with P-glycaprotein (Pgp), encoded by the multidrug resistance gene MDR1 and MRP1 drug transporters to circumvent the effect of these proteins conferring multidrug resistance and poor prognosis [6].

As most of the current anticancer agents are subject to multidrug-resistance efflux and are currently irreplaceable in several chemotherapy regimens, an attractive solution for improving response to therapy can therefore be the development of new classes of agents that do not interact with the multidrug ABC transporters. Interestingly, antitumoral properties of the nitrobenzofurazane derivative 6-(7-nitro-2,1,3-benzoxadiazol-4-ylthio)hexanol, which is a strong inhibitor of the GST family, has recently been reported [7]. GST catalyzes the conjugation with GSH of many anticancer drugs that can be efficiently removed from the cell by specific export pumps [8]. To date, no efficient and reliable cell-based methods have been designed to effectively monitor the cell's GSH/GSSG redox state and potential capacity as a target for a given chemotherapeutic drug.

Scanning Electrochemical Microscopy (SECM) is a well known technique that has been extensively used to study the topography and reactivity of surfaces in electrochemistry [9]. It can readily study electrochemical reactions occurring at biological interfaces (Bio-SECM), such as live cells using nanoscale electrodes. In the last decade, several cell lines have been successfully analyzed by SECM [10–17]. To establish SECM as a general method enabling one to

* Corresponding author at: Department of Chemistry, Université du Québec à Montréal, C.P. 8888, Succ. Centre-ville, Montréal, QC, Canada H3C 3P8. Tel.: +1 514 987 3000x0895; fax: +1 514 987 4054.
E-mail address: mauzeroll.janine@uqam.ca (J. Mauzeroll).

1567-5394/$ – see front matter © 2011 Elsevier B.V. All rights reserved.
doi:10.1016/j.bioelechem.2011.04.008

quantify the extent of multidrug resistance in cancer cells, it is mandatory to first identify a pair of mediators that are cell permeable/impermeable and that interact with a specific major cell constituent that is affected by multidrug resistance. As such, we describe how electrochemical monitoring of ferrocenemethanol ($FcCH_2OH$) in human adenocarcinoma cervical cancer cells HeLa and in a multidrug resistant variant overexpressing MRP1 is related to the redox state of the cells through its interaction with the glutathione couple (GSH/GSSG). We demonstrate that the differential response to $FcCH_2OH$ in multidrug-resistant cells observed both through electrochemistry and flow cytometry is in part due to MRP1's unspecific efflux. This newly established relation between $FcCH_2OH$/$[FcCH_2OH]^+$, GSH/GSSG and multidrug resistance in human cancer cells enables the acquisition scanning electrochemical microscopy images, illustrating the possibility of a local quantification of GSH/GSSG released from resistant cancer cells.

2. Experimental

2.1. Cell culture

All products were purchased from Sigma-Aldrich (ON, Canada) if not indicated differently. HeLa (CCL-2, American Type Culture Collection, VA, USA) were grown in Dulbecco's Modified Eagle's Medium (DMEM high glucose, HyClone, UT, USA) completed with 10% v/v heat inactivated fetal bovine serum (Gibco/Invitrogen, ON, Canada), 2 mM glutamine, penicillin and streptomycin (50 units/ml) (HYQ HyClone, UT, USA), which was used as basic medium ($DMEM^+$). HeLa-R overexpress the Multidrug Resistance Protein 1 (MRP1) and are resistant to Actinomycin D, Etoposide, Adriamycin and Vincristine [18]. Cells were maintained in tissue culture flasks (Sarstedt Inc, QC, Canada) at 37 °C and 5% CO_2 using an CO_2/Multi-gas incubator (Sanjo Scientific, Japan). The culture medium for the HeLa-R contained Etoposide (VP-16, 250 ng/ml), which was removed prior to experiments [19]. Both cell lines, ranging from 70% to 90% confluence, were washed with 37 °C phosphate buffered saline (PBS) (pH 7.4 at 25 °C) and harvested with 37 °C 0.25% v/v Trypsin-Ethylenediaminetetraacetic acid (EDTA) solution (10×, 2.0 g EDTA, in 0.9 wt.% NaCl). Optical micrographs of platted cultured cells were acquired using an inverted microscope (Nikon Eclipse TS100) equipped with a camera (Olympus CAMEDIA C-500 ZOOM, using Gimp 2.4).

2.2. Membrane preparation and western blotting

MRP1 and Glyceraldehyde-3-phosphate dehydrogenase (GAPDH, Immuno Chemical, CA, USA) protein expression in HeLa and HeLa-R cells was detected by western blot analysis as described elsewhere [20]. The Bradford method was used for protein quantification of the cell lysates [21]. Membranes were further washed and incubated for 1 h at room temperature with TBS-Tween 0.3% v/v containing the MRP1 specific monoclonal antibody QCRL (1:100) (Abcam Inc, MA, USA) followed by an 1 h incubation period with horseradish peroxidase anti-mouse antibody (1:1000) (Amersham Pharmacia Biotech, Rainham, UK) in 1.0 wt.% skim milk in TBS-Tween 0.3% v/v. The same membranes were used to detect GAPDH as control protein. The GAPDH specific monoclonal antibody (1:10,000) in TBS-Tween 0.1% v/v + 3 wt.% bovine serum albumin (BSA) + 0.02 wt.% NaN_3 was exposed to the membranes for 20 min and protein detection and analysis was performed as described before for MRP1-QCRL detection (Also see supporting information).

2.3. Flow Cytometry

HeLa and HeLa-R cells were plated into 60-mm Petri dishes 24 h before experiment. Cells were washed with PBS and incubated in $DMEM^+$, $DMEM^-$ or PBS for different periods of time. To detect the intracellular GSH, cells were incubated 15 min in respective medium before 5-chloromethylfluorescein diacetate (CMFDA, Invitrogen, ON, Canada) was added in concentrations ranging from zero to 2.5 μM. CMFDA was dissolved and diluted in dimethyl sulfoxide (DMSO). Cells were incubated in respective medium containing CMFDA for another 15 min, washed with PBS and harvested with a 37 °C Trypsin solution. Trypsin solution was removed by centrifugation at 1000 *g* for 5 min. Cells were resuspended in 0.5 ml $DMEM^+$. Flow cytometric measurements were performed using FACSCalibur (BD Bioscience, USA) and data was analyzed with the software WinMDI (Windows Multiple Document Interface for Flow Cytometry, version 2.8). $FcCH_2OH$ and hexaammineruthenium(III) chloride ($[Ru(NH_3)_6]^{3+}$), both in 1 mM concentrations, were used respectively as cell permeable and impermeable electrochemical probes. Simultaneously, cell death was monitored using 0.02 mg/ml PI solution (EMD Chemicals, NJ, USA).

2.4. Preparation of the control strain of HeLa cells before the electrochemical analysis

HeLa cells (ATCC, VA, USA) were seeded on 25-mm polymer disks (NUNC Brand Thermanox) or 23 mm Zeonor 1060R (Zeon Chemicals, KY, USA) oxygen plasma-treated (40 W/sccm) disks, 24 h prior to measurements [22]. The day of the analysis, the cells were washed with PBS and put in the corresponding redox solution.

2.5. Bulk electrolysis of $FcCH_2OH$ into $[FcCH_2OH]^+$ and exposure of HeLa cells to $[FcCH_2OH]^+$

Bulk electrolysis of $FcCH_2OH$ (1 mM dissolved in Minimum Essential Medium (MEM−)) into its ferrocenium cation ($[FcCH_2OH]^+$) was achieved using a platinum sheet working electrode, an galvanized steel control electrode contained in a fritted glass tube and an Ag/AgCl reference electrode placed in a three-chamber electrolysis cell. Oxidation of $FcCH_2OH$ was performed by applying 0.4 V constant voltage for 3 h and resulted in a calculated faradaic efficiency of 0.94. Following bulk electrolysis, the stability of the ferrocenium cation solution is maintained for at least 12 h, which is long enough for its use in HeLa cells studies.

The effect of $[FcCH_2OH]^+$ on HeLa cells was evaluated by CMFDA fluorescence intensity. Cells were washed with PBS and incubated for 15 min in MEM− for the control group and MEM− containing $[FcCH_2OH]^+$ for the tested group. Both groups were then stained with 2 μM CMFDA for 15 min, rinsed with PBS and then placed in MEM− prior to acquisition. Fluorescence micrographs were acquired using a Nikon Eclipse TE2000-U inverted microscope equipped with a FITC/RSGFP/Bodipy/Fluo 3/DiO filter # 41001 (Chroma Technology, VT, USA) using a Retiga 2000R Fast 1394 Mono Cooled CCD camera (Qimaging, BC, Canada).

2.6. Biological SECM measurements on HeLa cells

2.6.1. Electrodes

A three-electrode setup was used for voltammetry and SECM experiments with 25 micrometer platinum (Pt) diameter or laser pulled Pt working electrodes, a Ag/AgCl (3 M NaCl) pseudo-reference electrode (calibrated in $FcCH_2OH$) and 0.5 mm Pt auxiliary. The preparation of conventional 25 micrometer Pt microelectrodes followed a well established fabrication protocol [23] while polished; needle-like, disk-shaped nanoelectrodes were fabricated using a similar to the procedures described [24]. The fabrication procedure specifically produces disk shaped Pt microelectrode sealed in a quartz capillary and laser pulled until a dimensionless radius of glass (RG) inferior to 10 is obtained. In brief, 25 μm annealed Pt wires were pulled into quartz glass capillaries (length of 150 mm, an outer diameter of 1 mm, and an inner diameter of 0.3 mm) under vacuum with the

help of a P-2000 laser pipet puller (Sutter Instruments, CA, USA). The pulling program results in the formation of a long and sharp microelectrode with a thin glass sheath, which facilitates membrane penetration. The effective radius was evaluated from steady-state voltammetry.

2.6.2. Electrochemical measurements

The Biological Scanning Electrochemical Microscope is an instrument that consists of a SECM apparatus combined with an optical microscope. The phase contrast microscope allows the exact positioning of a micro or nanoscale electrode above an area of interest containing cells. Prior to analysis, the microelectrode is electrochemically cleaned using cyclic voltammetry in H_2SO_4 (0.5 M) between −0.3 V and 1.5 V during 20 cycles, rinsed and dried. For the measurements in ($[Ru(NH_3)_6]^{3+}$) (1 mM dissolved in PBS), a probe approach curve at a speed of 1 μm/s was acquired above the immobilized HeLa cells exposed to ($[Ru(NH_3)_6]^{3+}$). A −0.35 V vs. Ag/AgCl potential was applied at the microelectrode in order to obtain an electrochemical image of the ($[Ru(NH_3)_6]^{3+}$) (III) reduction to ($[Ru(NH_3)_6]^{2+}$) (II). For the $FcCH_2OH$ (1 mM dissolved in MEM−), a probe approach curve was recorded at a speed of 1 μm/s above the cells using a 25 μm diameter Pt microelectrode following 70 min of exposition to $FcCH_2OH$. A 0.4 V vs. Ag/AgCl potential was applied at the electrode to obtain an electrochemical image of the $FcCH_2OH$ oxidation to $[FcCH_2OH]^+$. Finally, probe approach curves of a Pt microelectrode biased at 0.4 V vs. Ag/AgCl were recorded across the cell membrane of single HeLa cells that had been exposed to $FcCH_2OH$ for 1 h. The presence and position of the target cells has been monitored through the oculars of the optical microscope before and after the procedure.

2.7. Statistical analysis

All values were measured in triplicates and subsequently statistically evaluated. Based on a student's t-distribution, errors were calculated applying a two-tailed test with $n = 3$, $\alpha = 0.025$ and therefore a confidence level (CL) of 95% is given.

3. Results and discussion

3.1. Establishment of stringent cell culture and measuring conditions

HeLa and HeLa-R were used to study the influence of redox mediators on their intracellular thiol redox state using a combination of electrochemical and fluorescent techniques. Because the results obtained from both techniques are dependent on the cell metabolism, it is important to establish stringent cell culture and measuring conditions that prevent cell metabolism alterations that would bias the observed electrochemical and fluorescent measurements.

Electrochemical measurements must be performed in a non-disrupting media devoid of serum, such as Phosphate Buffered Saline (PBS), and Dulbecco's Modified Eagle Medium without serum ($DMEM^-$), in order to prevent electrode fouling. The influence of such culture media on the morphology, viability and redox state of cells was studied on two cell lines that have intrinsically different distinct morphologies and resistance phenotypes: the human cervical adenocarcinoma HeLa cells (HeLa) and human cervical adenocarcinoma multidrug-resistant HeLa cells (HeLa-R). Adherent HeLa cells present a triangular shape (Fig. 1a) while adherent HeLa-R cells present a reduction in cytoplasmic volume, are spherical and grow in colonies (Fig. 1b) [25]. HeLa and HeLa-R cells also differ in their expression level of MRP1 (190 kDa) as confirmed by western blotting

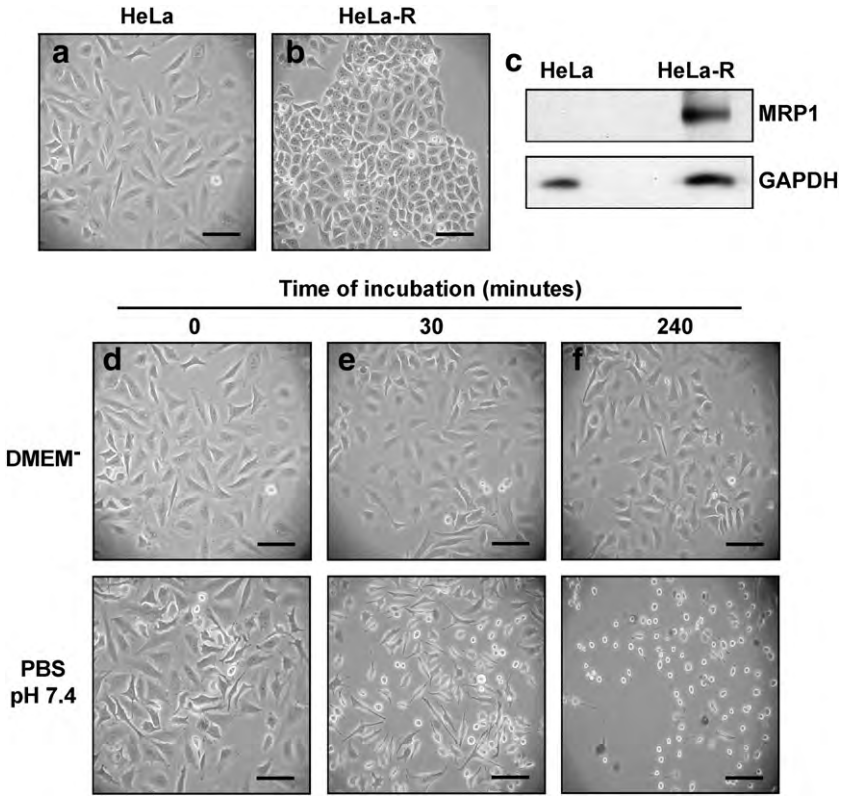

Fig. 1. Optical micrographs and western blot comparing both strains of HeLa cells. (a) HeLa cells in complete medium ($DMEM^+$). (b) HeLa-R cells in $DMEM^+$. (c) Western blot showing the constitutive expression of MRP1 protein in the multidrug resistant HeLa cells. The housekeeping gene GAPDH was used as a loading control. (d–f) Comparison of HeLa cells exposed to medium devoid of serum ($DMEM^-$) (upper panels) and PBS pH 7.4 (lower panels). Images were acquired after 0 min (d), 30 min (e) and 240 min (f) incubation. Scale bar for all micrographs correspond to 100 μm.

followed by immunodetection using a specific MRP1 monoclonal antibody (Fig. 1c). The housekeeping gene, glyceraldehyde-3-phosphate dehydrogenase (GAPDH, 36 kDa), was used as control protein and was expressed in both cell lines. The observed expression level of resistant protein and housekeeping gene are consistent with literature [18,26].

By varying the culture media the cell morphology changes incurred were studied by optical microscopy and flow cytometry. As presented in Fig. 1 (d–f, upper panels), prolonged exposure to PBS affects the HeLa cell morphology since cells separate and become globular. Although clearly stressed, the exposed HeLa cells do not detach from the culture dish and cell staining with Trypan blue confirmed that no excessive cell death occurred after 4 h of incubation in PBS. Even though the cells are not dying, the observed cytoskeletal perturbations are among early events leading to major metabolic changes [27,28]. In contrast, HeLa cells incubated in DMEM$^-$ show no external sign of stress (Fig. 1d–f, lower panels).

The optical microscopy measurements were corroborated and quantified by flow cytometry (Fig. 2a–d). The dot plot displaying the forward scattering signal and the side scattering signals is showing a focused distribution in DMEM$^-$ after an incubation of 2 h (Fig. 2a). A broadening of distribution occurs with increasing incubation period (Fig. 2c) or incubation in PBS (Fig. 2b, d). By taking the focused morphology distribution in DMEM$^-$ at 2 h incubation as reference, the percentage of cells with a similar morphology is calculated for all conditions (see supporting figure S1). In DMEM$^-$ 77.49% (67.87% in PBS) of all cells belong to the focused distribution after 2 h incubation period. After 4 h 64.05% (55.15% in PBS) of cells still hold a similar morphology. A similar effect was observed in HeLa-R cells (see supporting figure S2). These results demonstrate that incubation in DMEM$^-$ media, contrary to PBS, maintain the standard HeLa and HeLa-R cell morphology for up to 4 h.

The influence of culture media on the viability and metabolism of both cell lines was further studied by flow cytometric measurements that used propidium iodide (PI) and 5-chloromethylfluorescein diacetate (CMFDA) as fluorescent indicators of viability and intracellular thiol redox state (Fig. 3) [29]. The influence of the media on the dose response of CMFDA revealed potential limitations of substituting the preferred media, DMEM$^-$, by PBS. When both cell lines were incubated in DMEM$^-$ or PBS for 30 min at 37 °C and 5% CO_2, the CMFDA dose–response of the PBS incubated cells saturates as compared to that observed in DMEM$^-$ (Fig. 3). This effect is likely due to a higher permeability of the cell membrane caused by the alteration of cell osmolarity by PBS [30]. The cell viability remains nevertheless stable under both conditions and is in agreement with previous results (Fig. 1d–f).

The intracellular redox state of both cell lines is however significantly affected by PBS incubation. As such, incubation in DMEM$^-$ media is preferable to that in PBS because it sustains morphologically and metabolically representative HeLa and HeLa-R cells for up to 4 h. During this period, electrochemical measurements such as those presented in a subsequent section are thus expected to be representative of the normal behavior of each cell line.

3.2. Differential response of HeLa-R and HeLa cell to the presence of redox mediators

The differential behavior of HeLa-R and HeLa are studied by flow cytometry with CMFDA fluorescent staining, which binds to thiol groups and allows monitoring of intracellular glutathione homeostasis [31,32]. Fig. 4a shows a comparison of the dose–response of the CMFDA fluorescence signal in HeLa and HeLa-R cell lines. The CMFDA dose–response of the HeLa cells displays enhanced sensitivity as compared to that obtained with HeLa-R cells. This can be due to two

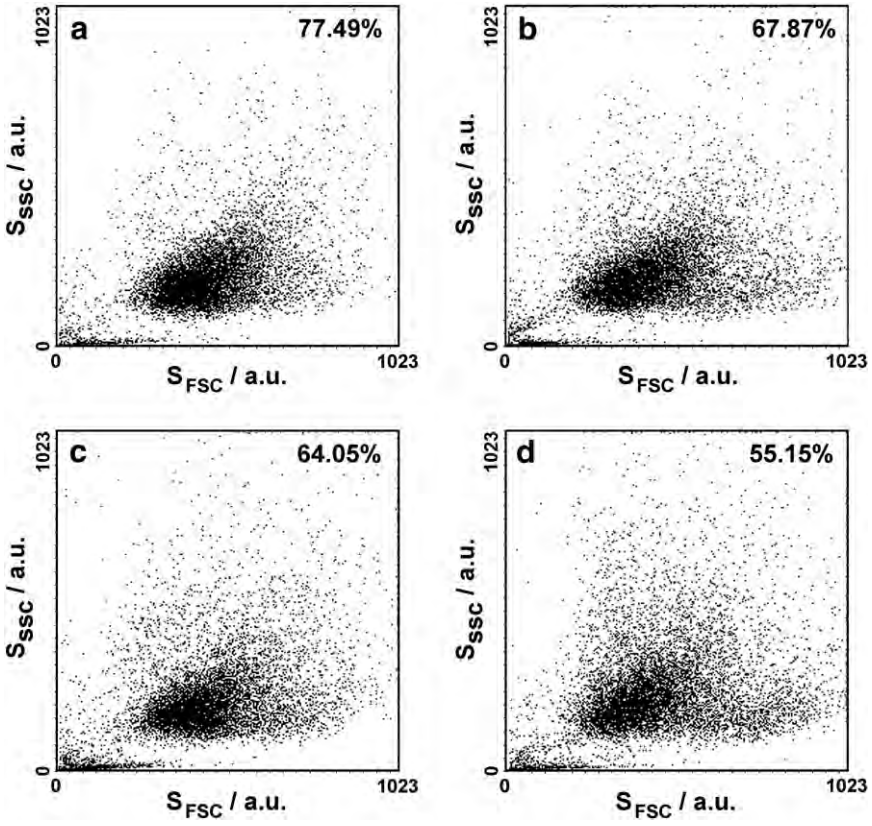

Fig. 2. Statistical validation of morphological changes in HeLa cells. (a) The dot plot displaying the forward (S_{FSC}) and side scattering (S_{SSC}) signals shows a focused distribution after 2 h in DMEM$^-$. Distribution broadening can be seen when cells are exposed to DMEM$^-$ for 4 h (c) or to PBS pH 7.4 during 2 h (b) and 4 h (d). Cell viability and the dose–response relationship between CMFDA concentration and cell fluorescence intensity is shown for cells exposed to DMEM$^-$ or PBS.

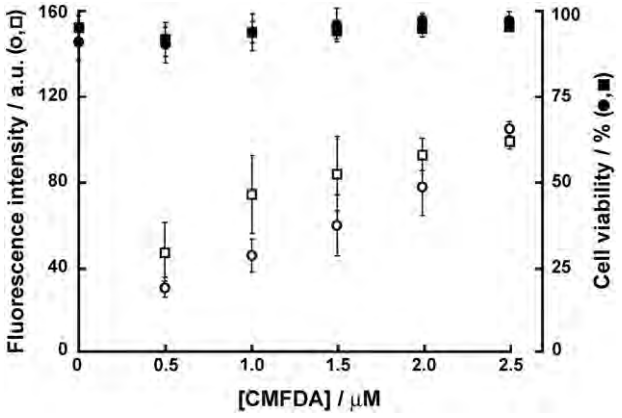

Fig. 3. Dose–response to CMFDA depending on cell medium. HeLa cells were incubated for 30 min in DMEM$^-$ (PI ●, CMFDA ○) or and in PBS pH 7.4 (PI ■, CMFDA □). Viability is defined as the ratio of numbers of viable cells to the total cell number (10,000).

major effects. First, it was previously shown that HeLa-R cells contain less intracellular glutathione as compared to HeLa cells [19]. Second, a fraction of CMFDA gets pumped out of the cell by MRP1 before it can react with thiol groups inside the cell. The dose–response of both cell lines displays a wide linear range from zero to 2.5 μM CMFDA. Finally, no substantial cell death was observed in the presence of CMFDA over this range based on propidium iodide fluorescence intensity (Fig. 4a). This result is in accordance with literature [33].

The interaction of two redox mediators: ferrocenemethanol ($FcCH_2OH$) and hexaammineruthenium(III) chloride ($[Ru(NH_3)_6]^{3+}$), was next assessed with HeLa and HeLa-R cells and their effect on the intracellular thiol redox state monitored by CMFDA fluorescence. The former is cell permeable [30] but its effect on cell metabolism and intracellular redox state remains unclear. The latter is a highly charged redox mediator that is cell impermeable [34] and serves as a negative control in Bio-SECM studies [10,13,34,35].

Under standard electrochemical conditions, no considerable cell death occurs in 1 mM $FcCH_2OH$/DMEM$^-$-treated cells (see supporting figure S3). HeLa cell incubation in $FcCH_2OH$ results in a statistically significant increase (confidence level (CL) 95%) in CMFDA fluorescence intensity (Fig. 4b). This indicates that the intracellular concentration of GSH is increased upon initial exposure to $FcCH_2OH$. In the HeLa-R cells, no statistically significant (CL 95%) fluorescence intensity shift is observed (Fig. 4c). This suggests that $FcCH_2OH$ is pumped out of the cell by MRP1, an indication that this mechanism acts unspecifically and actively. Incubation of both cells lines in the cell impermeable redox mediator ($[Ru(NH_3)_6]^{3+}$) did not result in significant (CL 95%) CMFDA fluorescence intensity increase (Fig. 4d).

Importantly, the increase in CMFDA fluorescence in the presence of $FcCH_2OH$ is a transient effect that is subject to the equilibrium dynamics of the reduced and oxidized glutathione ratio. Upon 30 min incubation in $FcCH_2OH$, a statistically significant (CL 95%) CMFDA fluorescence intensity increase in HeLa cells is observed. For $FcCH_2OH$ incubation periods exceeding 60 min, it is expected that the backward enzyme assisted reaction, responsible for maintaining the cells' redox state homeostasis, prevails (Fig. 5) [36].

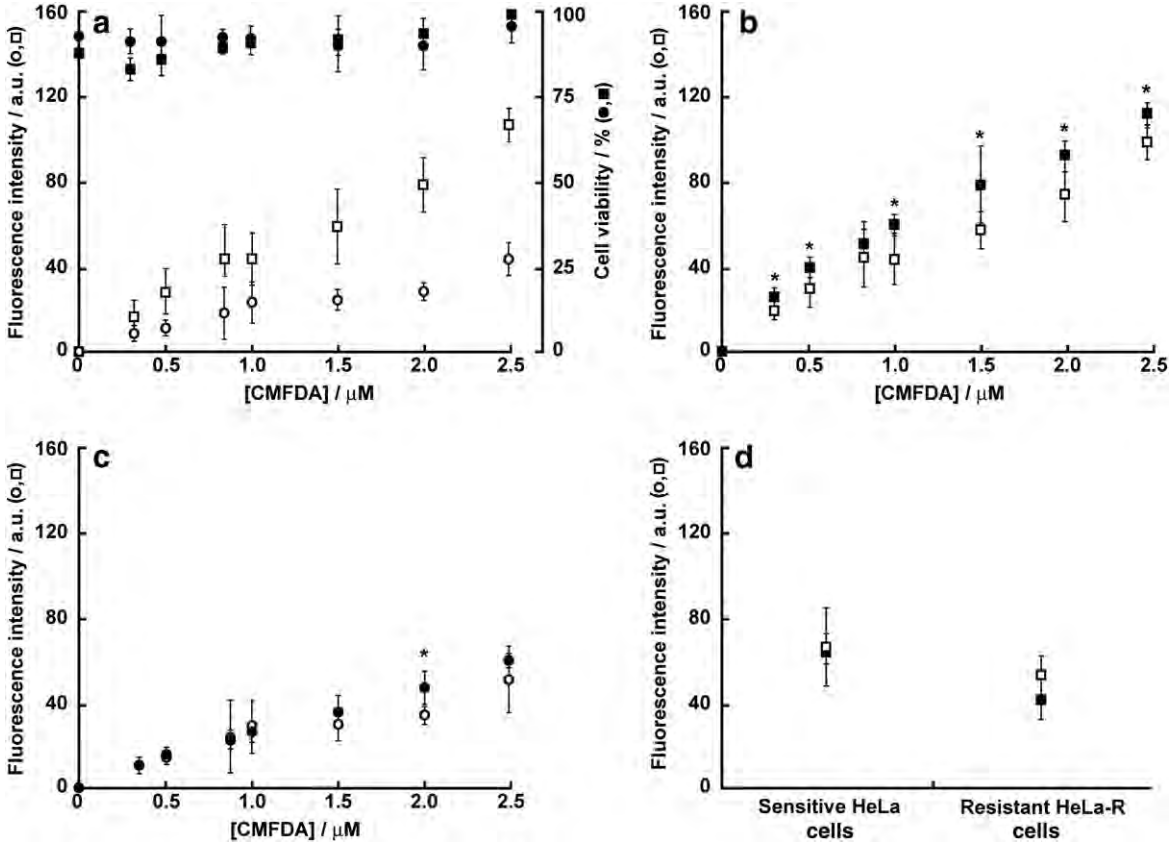

Fig. 4. Differential responses of cell lines to redox mediators. Cell viability and the dose–response relationship between CMFDA concentration and cell fluorescence intensity, obtained by flow cytometry, are shown for both cell strains exposed 30 min to D MEM$^-$. (a) HeLa (PI ■, CMFDA □) and HeLa-R (PI ●, CMFDA ○). (b–c) Dose–response relationship between different doses of CMFDA and its fluorescence intensity for the HeLa (b) and HeLa-R (c) cells incubated 30 min in either DMEM$^-$/1 mM $FcCH_2OH$ (■,●) or in DMEM$^-$ only (□,○). The asterisks correspond to a significant increase of fluorescence intensity ($n=3$; error bars representing the confidence interval of 95%) between groups exposed to DMEM$^-$/$FcCH_2OH$ and DMEM$^-$. (d) Flow cytometry fluorescence measurements in the presence of 2 μM CMFDA staining of both cell strains exposed 30 min to DMEM$^-$ containing (■) or not (□) 1 mM $[Ru(NH_3)_6]^{3+}$.

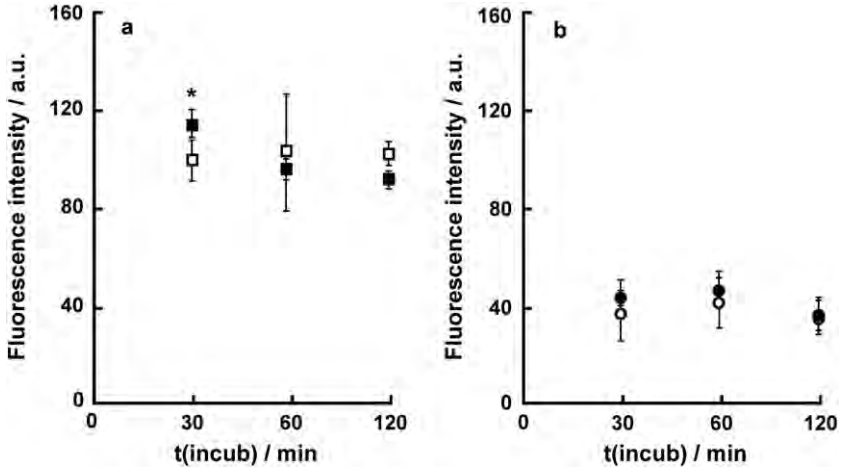

Fig. 5. Influence of $FcCH_2OH$ incubation time on CMFDA fluorescence intensity. HeLa (a) and HeLa-R (b) HeLa cells were exposed to 1 mM $FcCH_2OH$ in $DMEM^-$ for 30, 60 and 120 min (■,●) and compared to those only incubated in $DMEM^-$ (□,○). Flow cytometry fluorescence measurements of CMFDA (2.5 μM) added to the medium after 15, 45 or 105 min of incubation. The asterisks correspond to a significant difference ($n = 3$; error bars representing the confidence interval of CL 95%) between indicated groups.

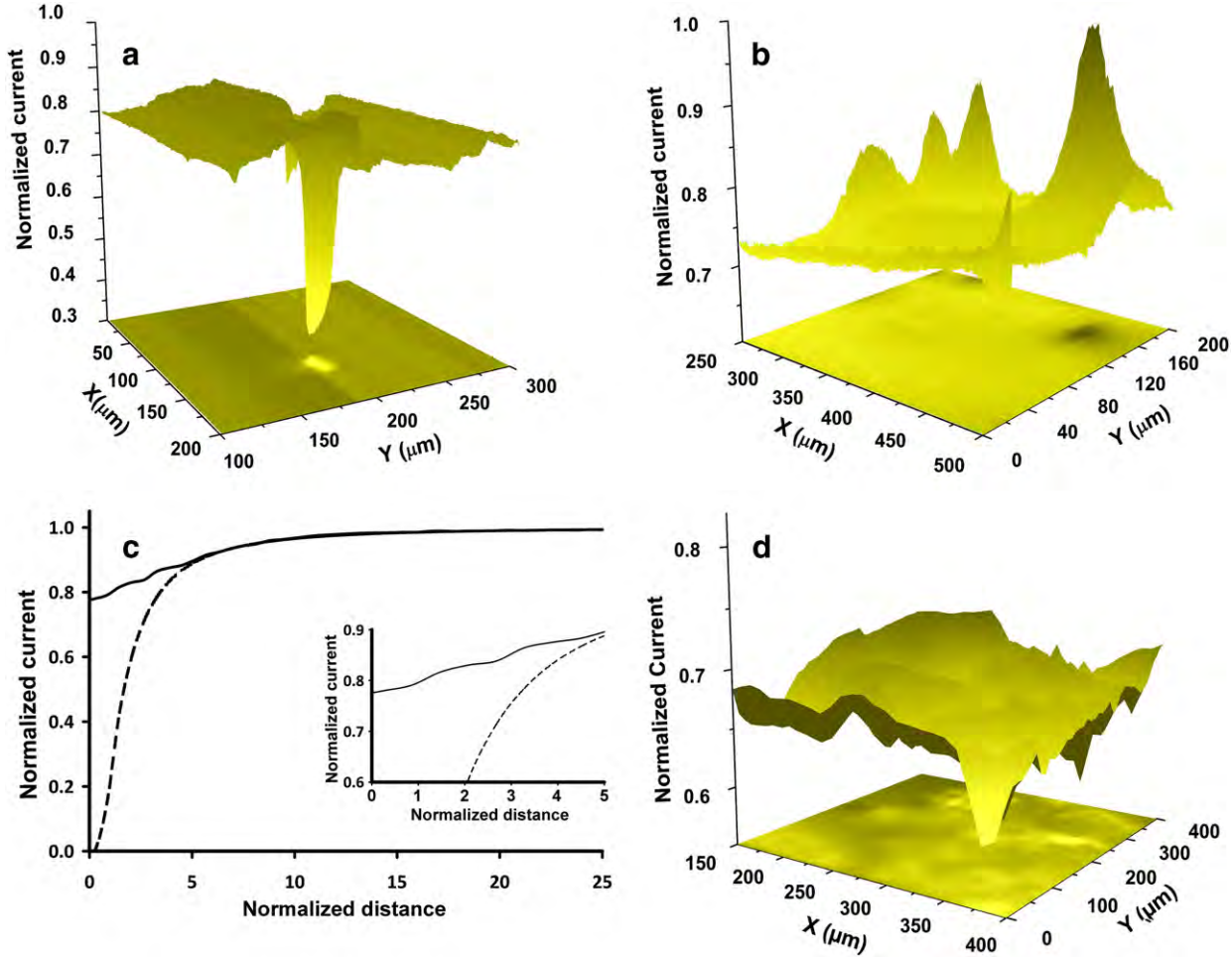

Fig. 6. (a) SECM electrochemical image of $[Ru(NH_3)_6]^{3+}$ (III) 1 mM reduction above HeLa cells. A – 0.35 V vs. Ag/AgCl potential was applied at the 1 μm diameter Pt microelectrode to reduce the $[Ru(NH_3)_6]^{3+}$ (III). Normalized current (current divided by current measured far from substrate) is presented for all images. (b) SECM electrochemical image the $FcCH_2OH$ oxidation to $[FcCH_2OH]^+$. SECM electrochemical image of $FcCH_2OH$ 1 mM above HeLa cells is shown. A 0.4 V vs. Ag/AgCl potential was applied at the 25 μm diameter Pt microelectrode to oxidize $FcCH_2OH$. (c) Approach curve in $FcCH_2OH$ 0.75 mM from above a HeLa cell (full line). Negative feedback theoretical curve (expression taken from literature [45] shows mismatch with experimental curve (see text). Pt microelectrode of about 340 nm diameter; applied potential more anodic than 0.4 V vs. Ag/AgCl. Normalized distance (distance divided by the radius of the tip's active part) is presented. (d) SECM electrochemical image of $FcCH_2OH$ 1 mM above HeLa-R cells. An 0.4 V vs. Ag/AgCl potential was applied at the 25 μm diameter Pt microelectrode to oxidize $FcCH_2OH$.

3.3. Differential response of Hela-R and Hela cells during electrochemical studies

To date, no efficient and reliable cell-based methods have been designed to effectively monitor the cell's GSH/GSSG redox state and potential capacity as a target for a given chemotherapeutic drug. The glutathione metabolism inside all cells of the human body is important for the cellular defense against reactive oxygen species (ROS). This major antioxidant tripeptide reacts non-enzymatically with radicals and acts as the electron donor for the reduction of peroxides [37]. Moreover glutathione is essential for cell proliferation and maintains the thiol redox potential in cells keeping sulfhydryl groups of proteins in the reduced form [38]. The detailed glutathione function, its metabolism and oxygen-reduction-pathways have been described previously [37,39–43]. Our finding that the mediator couple ($FcCH_2OH/[FcCH_2OH]^+$) interacts with the oxidized and reduced form of glutathione suggests that the couple can be used intracellularly and extracellularly to evaluate the cell's redox state by electrochemistry.

The response of both cell lines in presence of the previously used electrochemical species, ($[Ru(NH_3)_6]^{3+}$) and $FcCH_2OH$, has been further studied using SECM. Starting with HeLa cells, an electrochemical image of the cell in presence of ($[Ru(NH_3)_6]^{3+}$) was acquired. In this configuration, a decrease in the recorded cathodic current was observed, when the microelectrode is scanned across the HeLa cells (Fig. 6a). Since ($[Ru(NH_3)_6]^{3+}$) is a cell impermeable redox mediator, its diffusion to the surface of the microelectrode is hindered in close proximity to the cells and a decrease in reduction current is observed. These results are consistent with similar SECM studies [34,44]. This experiment illustrates that although the cells are exposed to PBS and therefore the membrane integrity is not fully maintained, as discussed previously (Fig. 3), during SECM mapping, we observe a decrease in current in the presence of ($[Ru(NH_3)_6]^{3+}$), proving that this redox mediator indeed does not interact with cells.

In order to perform experiments on living cells without interfering with their normal behavior and metabolism, target cells have not been exposed to two different kinds of mediators and the experimental sequence has been systematically kept below 4 h. Therefore Fig. 6 a–d shows independent experiments, which have been performed with different probes on different cell samples. For example, Fig. 6a has been obtained with a 25 μm diameter probe, whereas Fig. 6b used a 1 μm diameter probe. In each case, the probes adequately resolved the adhered cells.

The electrochemical image obtained when $FcCH_2OH$ is used as the mediator is presented in Fig. 6b. The observed response significantly differs from that obtained with $Ru(NH_3)_6]^{3+}$: an increase in anodic current is observed when the microelectrode is positioned above the cells. This current increase occurs because the microelectrode generates $[FcCH_2OH]^+$, which thereafter diffuses within the confined volume of the microelectrode and cell surface, and is regenerated by a cell component back to $FcCH_2OH$. This aspect has further been investigated by performing quantitative approach curves above a cell. Fig. 6c shows an experimental approach curve fitted to the pure negative feedback theoretical approach curve using an analytical approximation [45] that has been validated trough comparison with numerical simulations of pure negative feedback. The RG used for the calculation of the curve is 10. The zero distance position of the theoretical negative feedback curve has been adjusted for comparison with the experimental curve. As the microelectrode approaches the cell, the current decreases because of the hindered diffusion of $FcCH_2OH$ to the microelectrode active surface. This decrease in current does not correlate with pure negative feedback theory. Quantitatively in Fig. 6c, both curves would have been perfectly superimposed if no regeneration of mediator had occurred. It has been verified that changing the parameters in the theoretical formula (RG and zero distance position) in a realistic range does not improve the fit between the curves. One can mention that the increase of current observed in Fig. 6b does not imply that there must be an increase of current when performing an approach, as in Fig. 6c. It simply means that the current should be higher than that expected for negative feedback, at the same distance as that used for the lateral scan. Indeed, Fig. 6c confirms that pure negative feedback is not accurately fitting the experimental curve. The discrepancy between the pure negative feedback response and the experimental approach curve in the presence of $FcCH_2OH$ confirms the significant regeneration of the mediator during electrochemical imaging. This observation is in accordance with what has been observed in SECM literature [13].

In the past, the $FcCH_2OH$ regeneration has not been consistently observed in cases where the cells die during the experiments [14]. This indicates that the regeneration of $FcCH_2OH$ is related to an active process. The extent of $FcCH_2OH$ efflux is therefore potentially related to the resistant phenotype of the cells. To confirm this idea, electrochemical imaging in the presence of $FcCH_2OH$ above Hela-R cells has been carried out (Fig. 6d). When the microelectrode is rastered across the HeLa-R cells the observed response is very different from that observed using HeLa (Fig. 6c). A slight decrease in current is recorded above cells. The differential response between HeLa and Hela-R cells means that $FcCH_2OH$ glutathione efflux for resistant cells could be measured electrochemically using Bio-SECM leading to quantification of the extend of cell's resistance.

One has to underline that difference from negative feedback observed above HeLa cells (Fig. 6b and c) cannot be due to $[FcCH_2OH]^+$ release from cells. Indeed, in contrast to $FcCH_2OH$, which diffuses into cells, $[FcCH_2OH]^+$ is cell impermeable. This aspect is demonstrated in Fig. 7, that presents results from fluorescence microscopy experiments with CMFDA and a solution of $[FcCH_2OH]^+$ obtained through classical bulk electrolysis. Fig. 7 shows that there is no significant (CL 95%) difference between the fluorescence intensity of the HeLa cells exposed and unexposed to $[FcCH_2OH]^+$. If $[FcCH_2OH]^+$ had entered the cell, it would have reacted with GSH, as determined electrochemically elsewhere [46,47]. This would have reduced the available intracellular concentration of GSH that would

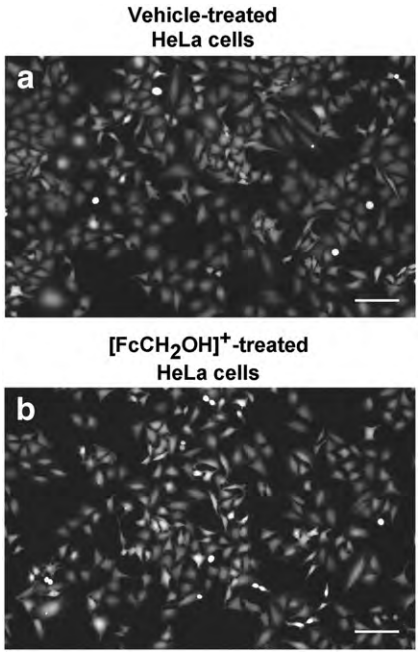

Fig. 7. Fluorescence images of HeLa cells. The fluorescence intensity of the unexposed HeLa cells (in $DMEM^-$; a) is compared to cells exposed to $[FcCH_2OH]^+$ in MEM− for 30 min (b). There is no substantial difference in the fluorescence intensity of the CMFDA. Micrographs were acquired using a Nikon Eclipse TE2000-U inverted microscope and Nikon NIS-Element software (version 3.0). Scale bar for all micrographs correspond to 100 μm.

have otherwise reacted with the CMFDA and resulted in a reduction in the fluorescence intensity as compared to that observed in the unexposed cells. Based on the present results, it appears that the charged species $[FcCH_2OH]^+$ is cell impermeable, and that the difference from negative feedback observed Fig. 6b and c cannot be explained by direct $[FcCH_2OH]^+$ cell release.

According to those results, it seems that differential response between HeLa and HeLa-R cells is likely to be related to the cell component, glutathione, responsible for the regeneration reaction using corroborating electrochemical and fluorescent experiments. Exact quantification of this differential response is however behind the scope of this preliminary study.

4. Conclusions

Using CMFDA as a fluorescent tag in flow cytometry, a relation between intracellular glutathione and $FcCH_2OH$ was found. The intensity of the CMFDA fluorescence response was dependent on the cells MRP1 expression. Bio-SECM confirmed the observed reactivity of HeLa cells towards $FcCH_2OH$ by exhibiting a positive contribution to the current. This could be explained by the fact that upon $FcCH_2OH$ stimulation, GSH is actively transported through MRP1 and reacts with the $[FcCH_2OH]^+$ produced at the probe electrode. The latter species however cannot penetrate the cell membrane, as shown by fluorescence microscopy. The establishment of the exact reaction mechanism is still under investigation. Our findings establish an important first step towards the quantification of multidrug resistance.

Given the nature of Bio-SECM and its hyphenation with fluorescence microscopy, the intracellular flux of $FcCH_2OH$ and extent of regeneration reaction of $[FcCH_2OH]^+$ will be used to relate multidrug resistance to ubiquitous glutathione. This could lead to the establishment of a quantifiable indicator for multidrug resistance activity that can be used over cell life and across cell lines thereby enabling targeted drug screening and improving existing chemotherapeutical treatments.

Supplementary materials related to this article can be found online at doi:10.1016/j.bioelechem.2011.04.008.

Acknowledgements

JM and BA acknowledge the Natural Sciences and Engineering Research Council of Canada (NSERC) and the Canadian Foundation for Innovative (CFI) for their financial support. BA holds a Canada Research Chair in Molecular Oncology from the Canadian Institutes of Health Research (CIHR). The authors thank Dr. Philippe Gros (McGill University, Montreal) for providing the MRP1 overexpressing variant of the HeLa cells and Matthias Geissler (Industrial Materials Institute, NRC, Boucherville) for providing Zeonor disks. The technical contributions of M. Marion, Dr. Charles Cougnon and Chistian Kuss are also acknowledged.

References

[1] L.J. Goldstein, I. Pastan, M.M. Gottesman, Multidrug resistance in human cancer, Crit. Rev. Oncol. Hematol. 12 (1992) 243–253.
[2] A. Persidis, Cancer multidrug resistance, Nat. Biotechnol. 17 (1999) 94–95.
[3] C.E. Grant, G. Valdimarsson, D.R. Hipfner, K.C. Almquist, S.P.C. Cole, R.G. Deeley, Overexpression of multidrug resistance-associated protein (MRP) increases resistance to natural product drugs, Cancer Res. 54 (1994) 357–361.
[4] P. Borst, R. Evers, M. Kool, J. Wijnholds, A family of drug transporters: the multidrug resistance-associated proteins, J. Natl. Cancer Inst. 92 (2000) 1295–1302.
[5] C.S. Morrow, K.H. Cowan, Glutathione S-transferases and drug resistance, Cancer Cells 2 (1990) 15–22.
[6] A. Ascione, M. Cianfriglia, M.L. Dupuis, A. Mallano, A. Sau, T.F. Pellizzari, S. Pezzola, A.M. Caccuri, The glutathione S-transferase inhibitor 6-(7-nitro-2,1,3-benzoxadiazol-4-ylthio)hexanol overcomes the MDR1-P-glycoprotein and MRP1-mediated multidrug resistance in acute myeloid leukemia cells, Cancer Chemother. Pharmacol. 64 (2009) 419–424.
[7] G. Ricci, F. De Maria, G. Antonini, P. Turella, A. Bullo, L. Stella, G. Filomeni, G. Federici, A.M. Caccuri, 7-Nitro-2,1,3-benzoxadiazole derivatives, a new class of suicide inhibitors for glutathione S-transferases. Mechanism of action of potential anticancer drugs, J. Biol. Chem. 280 (2005) 26397–26405.
[8] E. Bakos, L. Homolya, Portrait of multifaceted transporter, the multidrug resistance-associated protein 1 (MRP1/ABCC1), Eur. J. Physiol. 453 (2007) 621–641.
[9] A.J. Bard, M.V. Mirkin, Scanning Electrochemical Microscopy, first ed. Marcel Dekker, Inc., New York, 2001.
[10] A.J. Bard, X. Li, W. Zhan, Chemical imaging living cells by scanning electrochemical microscopy, Biosens. Bioelectron. 22 (2006) 461–472.
[11] L.P. Bauermann, W. Schuhmann, A. Schulte, An advanced biological scanning electrochemical microscope (Bio-SECM) for studying individual living cells, Phys. Chem. Chem. Phys. 6 (2004) 4003–4008.
[12] T. Kaya, Y.S. Torisawa, D. Oyamatsu, M. Nishizawa, T. Matsue, Monitoring the cellular activity of a cultured single cell by scanning electrochemical microscopy (SECM). A comparison with fluorescence viability monitoring, Biosens. Bioelectron. 18 (2003) 1379–1383.
[13] X. Li, A.J. Bard, Scanning electrochemical microscopy of HeLa cells–effects of ferrocene methanol and silver ion, J. Electroanal. Chem. 628 (2009) 35–42.
[14] B. Liu, S.A. Rotenberg, M.V. Mirkin, Scanning electrochemical microscopy of living cells: different redox activities of nonmetastatic and metastatic human breast cells, Proc. Natl. Acad. Sci. U. S. A. 97 (2000) 9855–9860.
[15] J. Mauzeroll, A.J. Bard, Scanning electrochemical microscopy of menadione-glutathione conjugate export from yeast cells, Proc. Natl. Acad. Sci. U. S. A. 101 (2004) 7862–7867.
[16] J. Mauzeroll, A.J. Bard, O. Owhadian, T.J. Monks, Menadione metabolism to thiodione in hepatoblastoma by scanning electrochemical microscopy, Proc. Natl. Acad. Sci. U. S. A. 101 (2004) 17582–17587.
[17] T. Saito, C.C. Wu, H. Shiku, T. Yasukawa, M. Yokoo, T. Ito-Sasaki, H. Abe, H. Hoshi, T. Matsue, Oxygen consumption of cell suspension in a poly (dimethylsiloxane) (PDMS) microchannel estimated by scanning electrochemical microscopy, Analyst 131 (2006) 1006–1011.
[18] C. Kast, P. Gros, Epitope insertion favors a six transmembrane domain model for the carboxy-terminal portion of the multidrug resistance-associated protein, Biochemistry 37 (1998) 2305–2313.
[19] T. Souslova, D.A. Averill-Bates, Multidrug-resistant HeLa cells overexpressing MRP1 exhibit sensitivity to cell killing by hyperthermia: interactions with etoposide, Int. J. Radiat. Oncol. Biol. Phys. 60 (2004) 1538–1551.
[20] A. Sina, S. Lord-Dufour, B. Annabi, Cell-based evidence for aminopeptidase N/CD13 inhibitor actinonin targeting of MT1-MMP-mediated proMMP-2 activation, Cancer Lett. 279 (2009) 171–176.
[21] M.M. Bradford, A rapid and sensitive method for the quantitation of microgram quantities of protein utilizing the principle of protein-dye binding, Anal. Biochem. 72 (1976) 248–254.
[22] I. Beaulieu, M. Geissler, J. Mauzeroll, Oxygen plasma treatment of polystyrene and zeonor: substrates for adhesion of patterned cells, Langmuir 25 (2009) 7169–7176.
[23] F.-R.F. Fan, J. Fernandez, B. Liu, J. Mauzeroll, C.G. Zoski, Platinum and gold inlaid disks ≥ 5 μm diameter, in: C.G. Zoski (Ed.), Handbook of Electrochemistry, Elsevier B.V, Amsterdam, 2007, pp. 189–199.
[24] J. Mauzeroll, R.J. LeSuer, Laser-pulled ultramicroelectrodes, in: C.G. Zoski (Ed.), Handbook of Electrochemistry, Elsevier B.V, Amsterdam, 2007, pp. 199–211.
[25] T.T. Puck, P.I. Marcus, S.J. Cieciura, Clonal growth of mammalian cells in vitro growth characteristics of colonies from single HeLa cells with and without a "feeder" layer, J. Exp. Med. 103 (1956) 273–284.
[26] R.D. Barber, D.W. Harmer, R.A. Coleman, B.J. Clark, GAPDH as a housekeeping gene: analysis of GAPDH mRNA expression in a panel of 72 human tissues, Physiol. Genomics 21 (2005) 389–395.
[27] R.L. Bronaugh, S.W. Collier, J.E. Storm, R.F. Stewart, Invitro evaluation of skin absorption and metabolism, J. Toxicol. Cutaneous Ocul. Toxicol. 8 (1989) 453–467.
[28] J.K. Kamisato, M. Nowakowski, Morphological and biochemical alterations of macrophages produced by a glycan PSK, Immunopharmacology 16 (1988) 89–96.
[29] A. Longobardi Givan, Flow cytometry: first principles, first ed. Wiley-Liss, New York, 1992.
[30] N. Nakajima, Y. Ikada, Effect of solution osmotic pressure on cell fusion by poly (ethylene glycol), J. Bioact. Compatible Polym. 10 (1995) 14–27.
[31] D.W. Hedley, S. Chow, Evaluation of methods for measuring cellular glutathione content using flow cytometry, Cytometry 15 (1993) 349–358.
[32] D.W. Voehringer, D.J. McConkey, T.J. McDonnell, S. Brisbay, R.E. Meyn, Bcl-2 expression causes redistribution of glutathione to the nucleus, Proc. Natl. Acad. Sci. U. S. A. 95 (1998) 2956–2960.
[33] K. Mascotti, J. McCullough, S.R. Burger, HPC viability measurement: trypan blue versus acridine orange and propidium iodide, Transfusion 40 (2000) 693–696.
[34] P. Sun, F.O. Laforge, T.P. Abeyweera, S.A. Rotenberg, J. Carpino, M.V. Mirkin, Nanoelectrochemistry of mammalian cells, Proc. Natl. Acad. Sci. U. S. A. 105 (2008) 443–448.
[35] S. Amemiya, J. Guo, H. Xiong, D.A. Gross, Biological applications of scanning electrochemical microscopy: chemical imaging of single living cells and beyond, Anal. Bioanal. Chem. 386 (2006) 458–471.
[36] I.U. Schraufstatter, D.B. Hinshaw, P.A. Hyslop, R.G. Spragg, C.G. Cochrane, Glutathione cycle activity and pyridine nucleotide levels in oxidant-induced injury of cells, J. Clin. Invest. 76 (1985) 1131–1139.
[37] R. Dringen, Metabolism and functions of glutathione in brain, Prog. Neurobiol. 62 (2000) 649–671.

[38] I.A. Cotgreave, R.G. Gerdes, Recent trends in glutathione biochemistry–glutathione–protein interactions: a molecular link between oxidative stress and cell proliferation? Biochem. Biophys. Res. Commun. 242 (1998) 1–9.
[39] R.C. Lantz, R. Lemus, R.W. Lange, M.H. Karol, Rapid reduction of intracellular glutathione in human bronchial epithelial cells exposed to occupational levels of toluene diisocyanate, Toxicol. Sci. 60 (2001) 348–355.
[40] J. Markovic, C. Borras, A. Ortega, J. Sastre, J. Vina, F.V. Pallardo, Glutathione is recruited into the nucleus in early phases of cell proliferation, J. Biol. Chem. 282 (2007) 20416–20424.
[41] A. Meister, Glutathione-ascorbic acid antioxidant system in animals, J. Biol. Chem. 269 (1994) 9397–9400.
[42] A. Meister, Glutathione, ascorbate, and cellular protection, Cancer Res. 54 (1994) 1969–1969.
[43] W. Wang, N. Ballatori, Endogenous glutathione conjugates: occurrence and biological functions, Pharmacol. Rev. 50 (1998) 335–356.
[44] J. Mauzeroll, M. Buda, A.J. Bard, F. Prieto, M. Rueda, Detection of Tl (I) transport through a gramicidin-dioleoylphosphatidylcholine monolayer using the substrate generation-tip collection mode of scanning electrochemical microscopy, Langmuir 18 (2002) 9453–9461.
[45] R. Cornut, C. Lefrou, A unified new analytical approximation for negative feedback currents with a microdisk SECM tip, J. Electroanal. Chem. 608 (2007) 59–66.
[46] S.K. Schreyer, S.R. Mikkelsen, A synthetic cysteine oxidase based on a ferrocene-cyclodextrin conjugate, Bioconjug. Chem. 10 (1999) 464–469.
[47] S.A. Wring, J.P. Hart, B.J. Birch, Voltammetric behaviour of screen-printed carbon electrodes, chemically modified with selected mediators, and their application as sensors for the determination of reduced glutathione, Analyst 116 (1991) 123–129.

S. Kuss, M.Sc., is currently a Ph.D. student in the Mauzeroll research group.

R. Cornut, Ph.D., is a post-doctoral fellow in the Mauzeroll research group.

Isabelle Beaulieu, M.Sc., is currently a Technical Officer with the National Research Council of Canada at the Biotechnology Research Institute in Montreal.

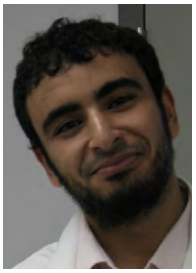

Mohamed A. Mezour, M.Sc., is currently a Ph.D. student in the Chemistry Department at McGill University in Montreal.

Borhane Annabi, Ph.D., is an associate professor and a Canada Research Chair in Molecular Oncology with the Chemistry Department at the University of Quebec in Montreal.

Janine Mauzeroll, Ph.D., is an associate professor with the Chemistry Department at the University of Quebec in Montreal.